Heliyon 11 (2025) e41589

Contents lists available at ScienceDirect

Heliyon

journal homepage: www.cell.com/heliyon

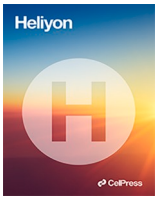

Research article

The potential synergistic effect of combining doxorubicin with vorinostat in urothelial carcinoma therapy

Cheng-Huang Shen [a,b,1], Shou-Chieh Wang [c,1], Kah-Min Lee [d], Hsin-Ting Liu [d], Szu-Wei Huang [e], Jin-Yi Wu [d], Yi-Wen Liu [d,*]

[a] *Department of Urology, Ditmanson Medical Foundation Chiayi Christian Hospital, Chiayi, 600, Taiwan*
[b] *SKBIO Technology Corporation, Taipei, 114065, Taiwan*
[c] *Division of Nephrology, Department of Internal Medicine, Kuang Tien General Hospital, Taichung, 437, Taiwan*
[d] *Department of Microbiology, Immunology and Biopharmaceuticals, College of Life Sciences, National Chiayi University, Chiayi City, Taiwan*
[e] *Department of Veterinary Medicine, College of Veterinary Medicine, National Chiayi University, Chiayi City, Taiwan*

ARTICLE INFO

Keywords:
Apoptosis
Bladder cancer
Doxorubicin
Synergistic effect
Vorinostat

ABSTRACT

Bladder cancer ranks as the 9th most common type of cancer worldwide. Approximately 70 % of bladder cancers are diagnosed as non-muscle invasive, and they are treated with transurethral resection followed by intravesical therapy. Doxorubicin is one of the effective cytotoxic drugs used in intravesical and systemic therapy, but its cardiotoxicity and nephrotoxicity limit therapeutic dosages. Vorinostat is an anticancer drug used to treat cutaneous T-cell lymphoma, and it demonstrates potent combination effects in various anticancer treatments. We aim to investigate the combined effects and mechanisms of doxorubicin and vorinostat in human bladder cancer cells. Human bladder cancer cells (5637 and BFTC 905) were used in this study. Cell viability of 5637 and BFTC 905 cells decreases in a time- and dose-dependent manner when treated with doxorubicin or vorinostat. Compared to the single drug treatment, the combination of doxorubicin and vorinostat synergistically induces cell death in 5637 and BFTC 905 cells. Combination drug treatment improves the expression of apoptosis-related proteins, including cleaved PARP, cleaved caspase 8, cleaved caspase 9, cleaved caspase-3, and γ-H2AX in both cell lines. Cell viability of combined treatment in both cell lines is partially restored by pre-treating with Z-VAD-FMK, a pan-caspase inhibitor. Z-VAD-FMK also completely reduced the protein expression of cleaved caspase 3 and γ-H2AX, suggesting that combining doxorubicin and vorinostat leads to DNA strand breaks and apoptosis. Pre-treatment with Z-IETD-FMK, a specific caspase 8 inhibitor, shows a slight recovery of cell viability in 5637 and BFTC 905 cells following combined treatment. Cleaved caspase 8, and γ-H2AX proteins in both cell lines are totally inhibited, and cleaved PARP is partially inhibited. Pre-treatment with Ac-LEHD-CMK, a specific caspase 9 inhibitor, no cell viability recovery in both cell lines. These results indicate that the combination of doxorubicin and vorinostat activates the caspase 8 and caspase 9 apoptosis pathways, and induces DNA strand breaks mainly via the caspase 8 pathway. The combination of doxorubicin and vorinostat also significantly inhibits the growth of BFTC 905 tumorspheres and BFTC 905 xenograft tumors in mice. In conclusion, our findings demonstrate that the combination of doxorubicin with

* Corresponding author. Department of Microbiology, Immunology and Biopharmaceuticals, College of Life Sciences, National Chiayi University, No. 300, Syuefu Rd, Chiayi City, 600, Taiwan.
E-mail address: ywlss@mail.ncyu.edu.tw (Y.-W. Liu).
[1] The two authors contributed equally to this work.

https://doi.org/10.1016/j.heliyon.2024.e41589
Received 27 August 2024; Received in revised form 24 November 2024; Accepted 30 December 2024
Available online 4 January 2025

vorinostat could potentially serve as a new treatment regimen for urothelial bladder cancer, for avoiding the high-dose side effect of doxorubicin.

Abbreviations

CIS	Carcinoma in situ
DMSO	Dimethyl sulfoxide
ER	Endoplasmic reticulum
FBS	Fetal bovine serum
HAT	Histone acetyltransferase
HDAC	Histone deacetylase
MIBC	Muscle-invasive bladder cancer
MPTP	Mitochondrial Permeability Transition Pore
NAC	*N*-acetylcystein
NMIBC	Non-muscle-invasive bladder cancer
PARP	Poly(ADP-ribose) polymerase
ROS	Reactive oxygen species
TBST	Tris-buffered saline with Tween 20

1. Introduction

According to the Globocan 2022 report of WHO Global Cancer Observatory, bladder cancer ranks 9th in terms of incidence and 13th in terms of mortality among all types of cancer worldwide [1]. The tumor stage is determined as a measure of the depth of bladder wall invasion. Tumors isolated from the urothelium (stage Ta) and from the lamina propria (stage T1) belong to non-muscle-invasive bladder cancer (NMIBC), while tumors that invade the muscle (stage T2) or extend beyond the muscle (stages T3 and T4) are classified as muscle-invasive bladder cancer (MIBC). Carcinoma in situ (CIS) is a distinct phenotype characterized by a high-grade flat noninvasive lesion with particularly high rates of recurrence and progression. In patients with low- and intermediate-risk NMIBC, the 5-year recurrence-free survival rates are 43 % and 33 %, respectively. About 21 % of high-risk NMIBC patients will progress to MIBC which needs aggressive therapy, including systemic chemotherapy [2]. In patients with nonmetastatic and metastatic MIBC, doxorubicin is always included in the chemotherapy regimen [2]. Therefore, the anti-cancer drug doxorubicin is used in the analysis of drug combinations in this project.

Doxorubicin, an anthracycline antibiotic, is a potent anti-cancer drug used to treat a wide variety of cancers. There are two different moieties in its structure, including an aglycone moiety and a daunosamine. The aglycone moiety consists of tetracyclic rings (anthraquinone) with the function of intercalating into DNA, leading to disruption of DNA repair [3]. In fact, the anti-cancer mechanisms of doxorubicin are diverse. They include the intercalation of DNA, inhibition of topoisomerase II, the production of free radicals via the quinone-semiquinone cycle [3] and NADPH-oxidase activation, interference with calcium homeostasis, and increases Mitochondrial Permeability Transition Pore (MPTP) permeability [3]. Despite its extensive clinical use in cancer treatment, doxorubicin has a major side effect: cardiotoxicity, which limits the dosage that can be used in patients [4]. Doxorubicin-induced chronic cardiotoxicity manifests as congestive heart failure, and the incidence increases with higher cumulative doses [5]; therefore, combining drugs offers a potential solution for reducing the cumulative dosage of doxorubicin.

DNA epigenetic modification is one of the important factors in cancer progression. Epigenetic modifications alter chromatin structure and DNA accessibility, which in turn affects gene expression patterns. Histone N-terminal tail acetylation is an epigenetic modification regulated by histone deacetylases (HDACs) and histone acetyltransferases (HATs) [6]. Deacetylation of histones leads to chromatin condensation, while increased acetylation causes decondensation [7]. Such changes might result in decreased or increased gene transcription. Histone deacetylases are important enzymes for maintaining histone deacetylation. It is known that HDACs are often dysregulated in cancers, making them a target for cancer therapeutic strategies. In various cancer cells, the alteration of the acetylation/deacetylation ratio through HDAC inhibition was found to have a significant impact on their fate [8]. The targeted epigenetic therapy of HDAC inhibition influences gene expression and ultimately controls tumor growth and proliferation. There are several chemical families in HDAC inhibition, including short-chain fatty acids (butyrate, valproic acid), hydroxamates (vorinostat, trichostatin A), cyclic tetrapeptides (depsipeptide), and benzamides (MS-275, MGCD-0103) [9]. Vorinostat is the first HDAC inhibitor to receive FDA approval for the treatment of cutaneous T-cell lymphoma in 2006. It is a pan-HDAC inhibitor that inhibits HDAC class I, II, and IV [8], and also suppresses the acetylation of other non-histone proteins, such as p53 [10]. Furthermore, through HDAC inhibition, vorinostat could decrease RAD51 expression by inducing microRNA-182, which impairs homologous recombination repair in acute myelogenous leukemia [11]. Resistance to HDAC inhibitors is frequently observed, and the success of HDAC inhibitors in treating solid tumors [6] including recurrent or metastatic transitional cell carcinoma, has been limited [12]. It has been reported that the combination of vorinostat and certain anti-cancer drugs produces a synergistic effect. For example, it has been shown to enhance

the effects of cisplatin [13], etoposide [14], epirubicin [15], and gefitinib [16]. Therefore, combining HDAC inhibitors with other anti-cancer drugs is a promising approach to achieving improved therapeutic outcomes.

Vorinostat, an HDAC inhibitor used in anti-cancer treatment, has a different mechanism of action compared to doxorubicin. The combination of vorinostat and other drugs may enhance the anti-cancer effect. In this study, we combined vorinostat and doxorubicin for the treatment of bladder cancer in both in vitro and in vivo.

2. Materials and methods

2.1. Cell culture

Human urothelial bladder cancer cell lines 5637 (BCRC60061) and BFTC 905 (BCRC60068) were purchased from Bioresource Collection and Research Center (BCRC, Hsinchu, Taiwan). Cells were cultured in RPMI 1640 medium supplemented with 10 % fetal bovine serum (FBS; Gibco, Mexico), 1 % penicillin/streptomycin (Gibco, USA) at 37 °C with 5 % CO_2. 5637 cells required extra supplement of 1 % 100 mM sodium pyruvate (Gibco, China) and 1 % 2 mM L-glutamine (Gibco, Brazil). Human urinary tract epithelial cell line SV-HUC-1 (BCRC60358) was purchased from BCRC and cultured in Ham's F12 medium supplemented with 7 % FBS and 1 % penicillin/streptomycin.

2.2. Chemicals

Doxorubicin was purchased from Hospira Australia Phy Ltd (Pfizer, Milano, Italy). Suberoylanilindehydroxamic acid (vorinostat) were acquired from ChemedEX (USA). Ac-LEHD-CMK was purchased from Santa Cruz Biotechnology (Santa Cruz, Dallas, Texas). *N*-Acetyl-L-cysteine (NAC) was acquired from Sigma-Aldrich. Z-IETD-FMK and Z-VAD-FMK were purchased from TargetMol (MA, USA). Doxorubicin and NAC were dissolved in sterile water at stock concentration of 5 mM and 500 mM respectively. Vorinostat were dissolved in dimethyl sulfoxide (DMSO) at stock concentration of 100 mM. Z-VAD-FMK, Z-IETD-FMK, and Ac-LEHD-CMK were dissolved in DMSO at stock concentration of 40 mM.

2.3. Cell viability assay

Cell viability was performed using 3-(4,5-dimethylthiazol-2-yl)-2,5-Diphenyltetrazolium (MTT; USB, Austria). 5637 cells or BFTC 905 cells were plated at 24-well plate in a final volume of 500 μl which treated with doxorubicin and/or vorinostat at the indicated concentrations for 24, 48 and 72 h. Briefly, 25 μl of MTT stock solution (5 mg/ml in phosphate-buffered saline) was added to each well, followed by incubation at 37 °C for 1 h to allow the cell-mediated reduction of MTT. To detect the amount of reduced MTT, 200 μl of dimethyl sulfoxide was added, and the absorbance was measured at 540 nm using ELISA reader. SV-HUC1 cells were plated at 96-well plate in a final volume of 100 μl which was treated with doxorubicin and/or vorinostat at the indicated concentrations for 24, 48 and 72 h. Ten μl of MTT stock solution was added to each well, followed by incubation at 37 °C for 3 h to allow MTT reduction. One hundred μl of dimethyl sulfoxide was added, and the absorbance was measured. The results were expressed as a percentage of MTT reduction in drugs-treated group compared with control group (100 %) for the drug alone or combined treatment group.

2.4. Evaluation of the synergistic, additive or antagonistic effect of two combined drugs

The effect of doxorubicin in combination with vorinostat was evaluated as originally described by Ting-Chao Chou [17]. Combination Index (CI) values were calculated from 15 different combinations of the two drugs via Compusyn software (www.combosyn.com; version 1.0, 2004 by Ting-Chao Chou and Nick Martin). $CI < 0.90$ indicates synergism, $CI = 0.90–1.10$ indicates addition, and $CI > 1.10$ indicates antagonism.

2.5. Western blot assay

After the treatment, the medium was aspirated. Total proteins from cells were extracted using PRO-PREP protein extraction solution (iNtRON Biotechnology Inc, Korea) supplemented with sodium fluoride (Honeywell Riedel-de-Haen, USA) and sodium orthovanadate (Sigma-Aldrich, USA). The protein concentration was determined using the bicinchoninic acid assay (Thermo scientific, USA). 15 μg total protein was fractionated on a 10%–15 % SDS-PAGE, and then electrophoretically transferred to a PVDF membrane (GE Healthcare Life Sciences, Germany) with Trans-Blot SD Semi-Dry Transfer apparatus (PIERCE G2 faster blotter; Thermo scientific). Membranes were blocked with Tris-buffered saline with Tween 20 (TBST) containing 5 % non-fat milk for 1 h at room temperature to minimize nonspecific binding. Membranes were incubated with primary antibodies at 4 °C overnight. After incubation with horseradish peroxidase-conjugated secondary antibody, blots were detected using an ECL detection reagent (Thermo scientific or Michigan Diagnostics). Each experiment was repeated at least 3 times. β-Actin was used as the loading control.

2.6. Antibodies for Western blot

Primary antibodies for β-actin (A5441; 1:10000) were purchased from Sigma-Aldrich (St. Louis, USA). Anti-caspase 8 (#9746; 1:1000), caspase 9 (#9502; 1:1000), cleaved caspase-3 (Asp 175) (#9661; 1:1000), and PARP (#9542; 1:1000) were purchased from

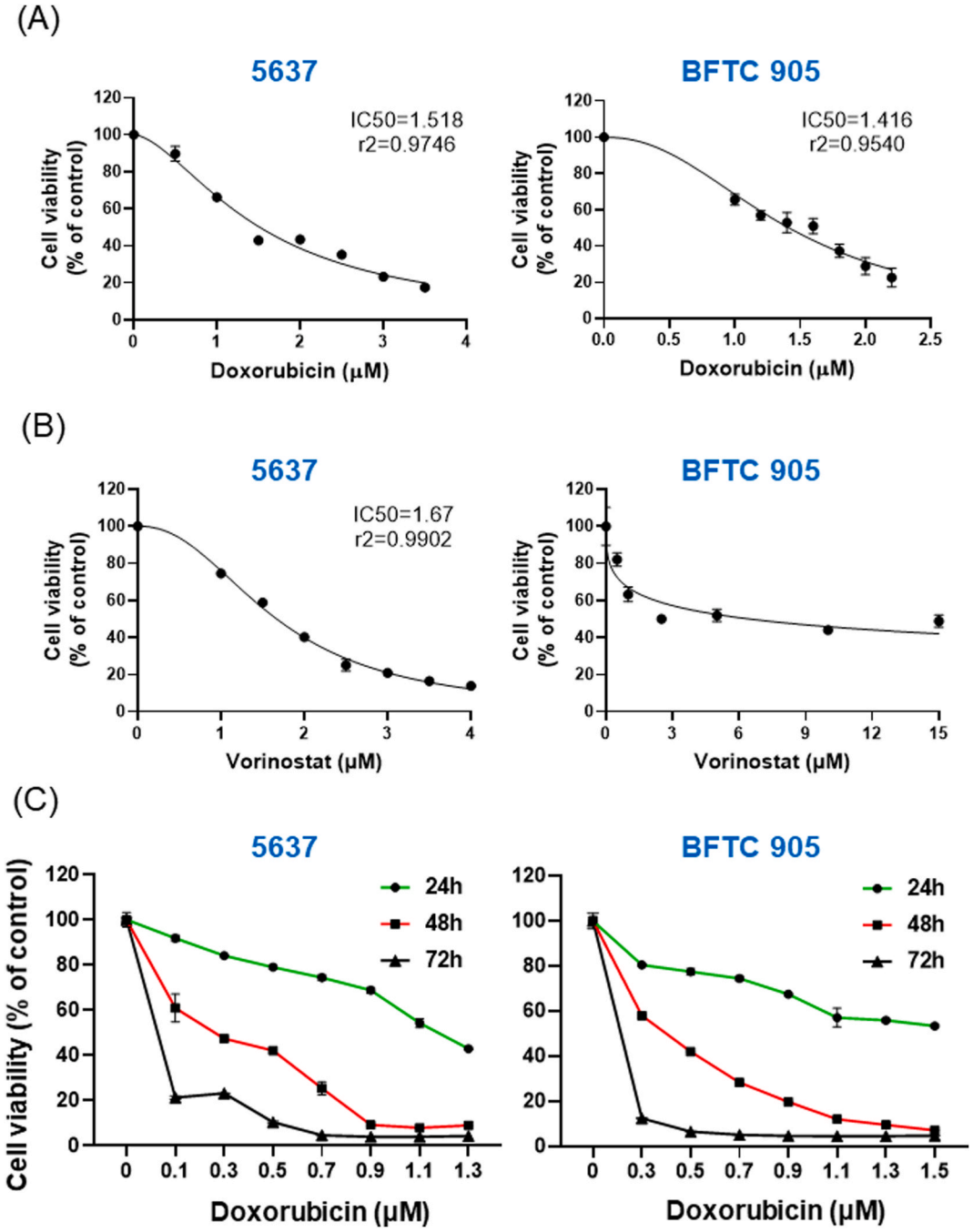

Fig. 1. Cytotoxicity of doxorubicin and vorinostat and their combination effect in 5637, BFTC 905 and SV-HUC-1 cells. (A) Cytotoxicity of doxorubicin for 24 h treatment. (B) Cytotoxicity of vorinostat for 24 h treatment. The IC50 and r2 values were calculated by nonlinear regression analysis of Prism 9. (C) Cytotoxicity of doxorubicin for 24, 48 and 72 h treatment. (D) Cytotoxicity of vorinostat for 24, 48 and 72 h treatment. (E) The combination effect of doxorubicin and vorinostat after 24 h treatment. The CI value in 5637 cells was calculated by the Compusyn software. (F) The combination effect of selected doses of doxorubicin and vorinostat (SAHA) after 24 h treatment in 5637 and BFTC 905 cells. (G) Cytotoxicity of combined drug treatment for 24, 48 and 72 h in 5637 and BFTC 905. (H) Cytotoxicity of single drug treatment for 24, 48 and 72 h in SV-HUC-1. (I) Cytotoxicity of combined 1.5 μM doxorubicin and 5 μM vorinostat for 24, 48 and 72 h treatment in SV-HUC-1.

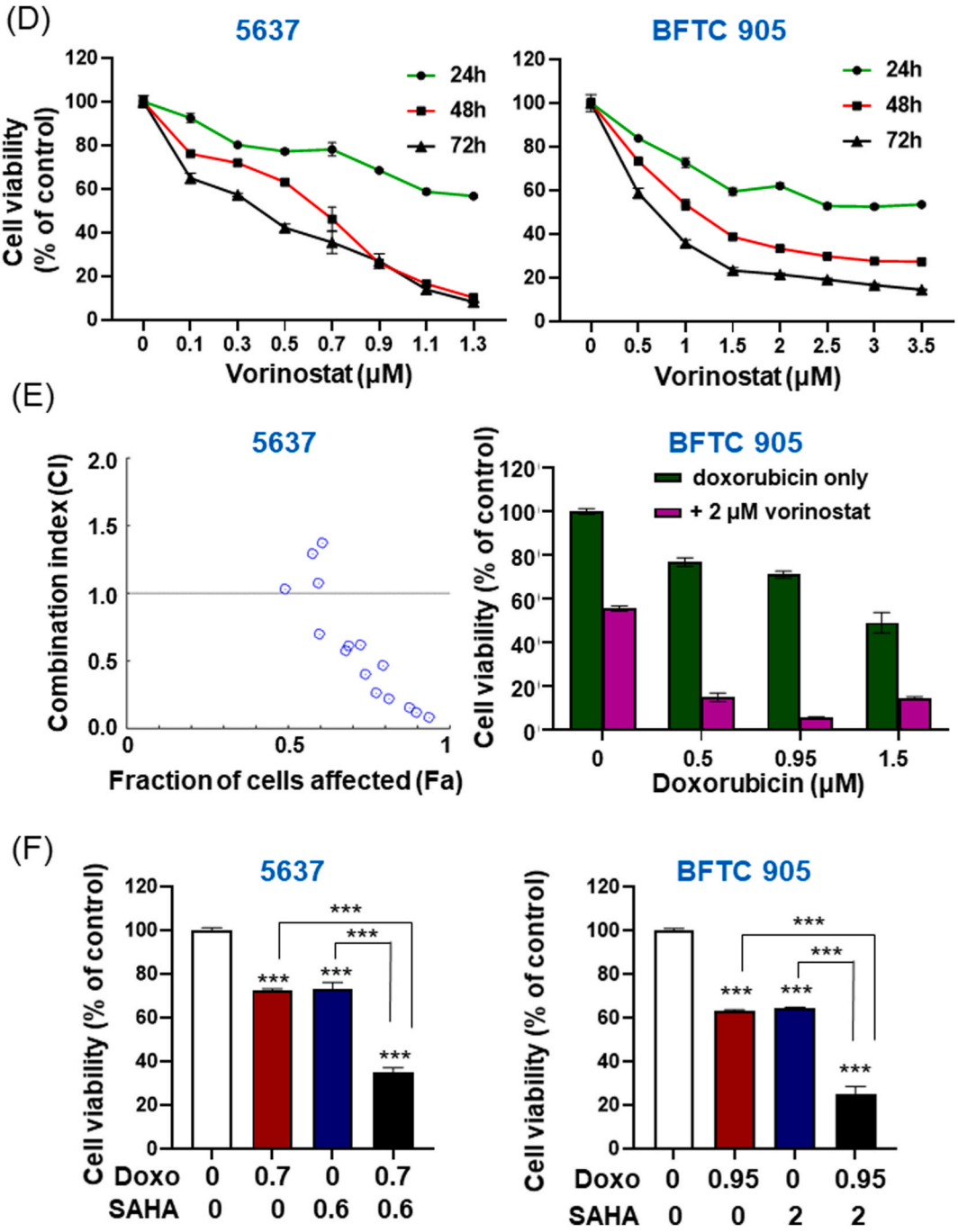

Fig. 1. (*continued*).

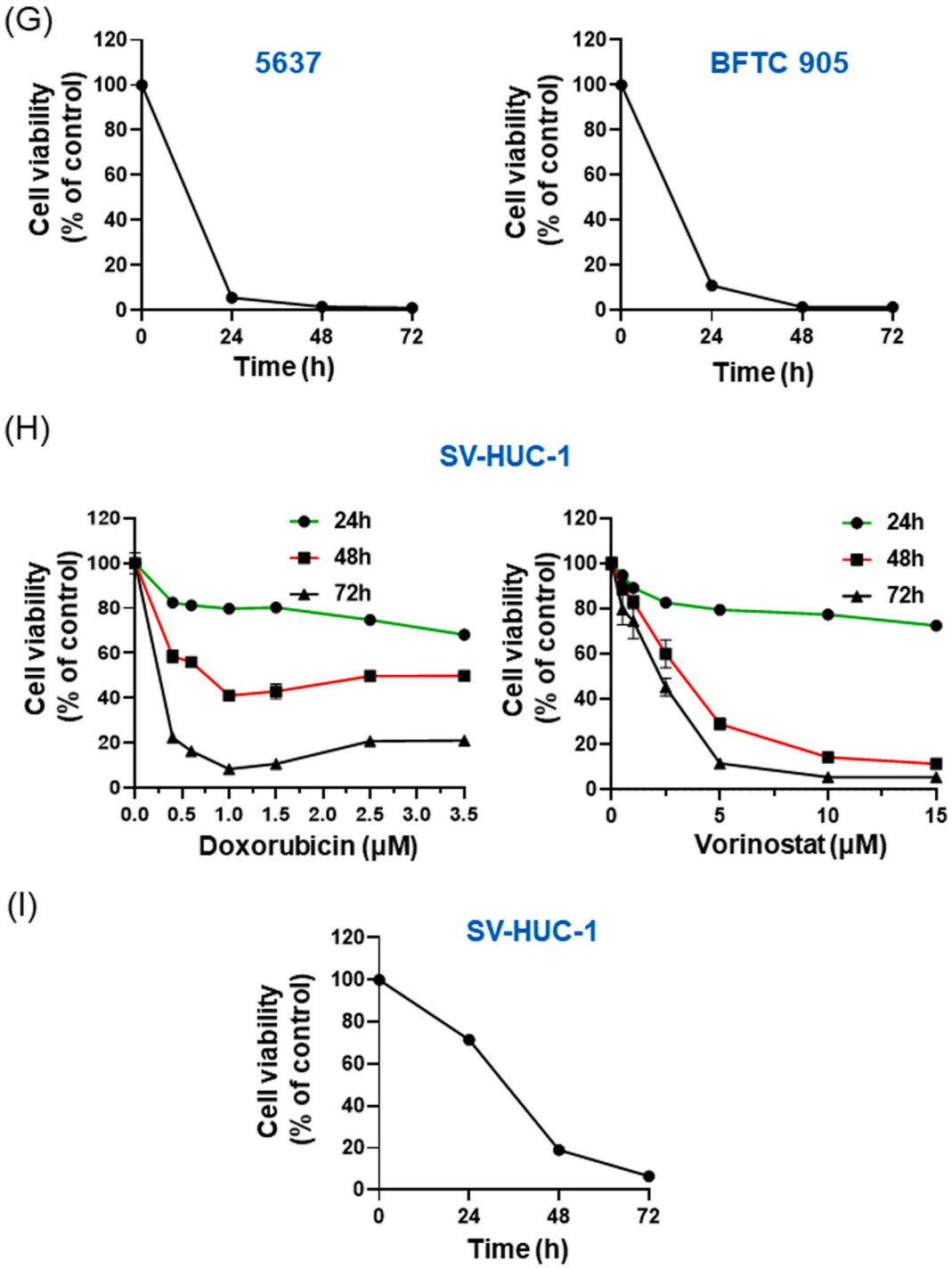

Fig. 1. (*continued*).

Cell Signaling Technology Inc (Danvers, MA, USA). Histone H2AX (phosphor-Ser139) (GTX127340; 1:1000) was obtained from GeneTex (MI, USA).

2.7. Incubation with various caspase inhibitors and ROS scavenger

5637 and BFTC 905 cells were pretreated with either the pan caspase inhibitor, Z-VAD-FMK (40 μM), caspase-8 inhibitor Z-IETD-FMK (40 μM), or caspase-9 inhibitor Ac-LEHD-CMK (40 μM), or ROS scavenger NAC (10 mM) for 1 h before doxorubicin or/and

vorinostat was added. Cell viaiblity was estimated using an MTT assay, then protein expression was determined by using Western blot.

2.8. Tumorspheres formation assay

BFTC 905 was seeded in 6-well ultra-low adherent plates (STEMCELL Technologies Inc, Canada) by MammoCult™ Human Medium Kit (STEMCELL Technologies Inc, 05620, Canada) supplemented with Heparin Solution (STEMCELL Technologies Inc, 07980, Canada) and Hydrocortisone Stock Solution (STEMCELL Technologies Inc, 07925, Canada) at a density of 4×10^4 cells/well. The volume of medium was maintained by adding 250 μl every 48 h. After 10 days, doxorubicin or/and vorinostat was treated to the formed tumorspheres. Doxorubicin and vorinostat were replenished with the 250 μl medium by every 48 h. Then, all groups of tumorspheres were photographed through microscopy and were counted (at least 70 tumorspheres in each group) for analysis.

2.9. In vivo xenograft anti-tumor study

Twenty-four 6-week-old NOD SCID female mice (National Laboratory Animal Center, National Applied Research Laboratories, Taiwan) were used in the in vivo study. The animal study protocol was approved by the Institutional Animal Care and Use Committee of National Chiayi University (No. 111048). All mice (body weight: 18–20 g) were maintained in a laminar airflow cabinet placed in a room maintained at 37.0 °C ± 0.5 °C and 40%–70 % relative humidity, with a 12-h light/dark cycle condition. Tumors were subcutaneously injected by 1×10^7 BFTC 905 cells which were mixed with the same volume of Matrigel® (Corning, product number 354234) into the right flanks of NOD SCID mice at day 0. Doxorubicin was dissolved in sterile water. Vorinostat was suspended in a buffer (10 % DMSO, 30 % polyethylene glycol 400, 5 % tween 80) and sonicated, then was centrifuged and filtered via 0.22 μm filter to get nanoparticles for injection. Animals were randomly divided into four groups (n = 6) at day 14 after tumor injection (day 0), which corresponding to the treatments with sterile water or buffer as control (group 1), doxorubicin treatment (group 2), vorinostat treatment (group 3), and doxorubicin-vorinostat combined treatment (group 4). The doses of doxorubicin and vorinostat administered were 1.8 mg/kg and 25 mg/kg of body mass respectively. Mice were intraperitoneally administered doxorubicin or water every 3 days up to a total number of 3 times (day14, 17 and 20), and vorinostat or buffer every day for a total number of 10 times (the last one was day 23). Weights and tumor volumes were carefully recorded throughout the period, and the diameter of tumors were measured by using a digital calliper. The tumor volume (mm^3) was calculated using the following formula: $[(width)^2 \text{ x } (lenght)]/2$. All mice were euthenized with CO_2 at day 27, and the tumors were excised for further analysis.

2.10. Statistical analysis

Data were analyzed using GraphPad Prism version 9 (GraphPad Software Inc., San Diego, USA). All results are expressed as the mean ± standard error (SE). The one-way ANOVA with Dunnett's multiple comparisons test was used when appropriate. A p-value <0.05 were considered statistically significant.

3. Results

3.1. Co-treatment with doxorubicin and vorinostat demonstrates synergistic cytotoxicity on human bladder cancer cells

The cell viability analysis was conducted to assess the effect of the combination of doxorubicin and vorinostat on cytotoxicity. In single-drug analysis, the 24-h treatment IC50 of doxorubicin was approximately 1.4–1.5 μM in 5637 and BFTC 905 cells (Fig. 1A),

Table 1
The effects and CI values of doxorubicin and vorinostat combination in 5637 cells.

Doxorubicin (μM)	Vorinostat (μM)	Effect	CI value	Interpretation[a]
0.4	0.8	0.49310	1.03073	+/−
	1.0	0.59928	0.69580	+++
	1.5	0.74112	0.40574	+++
	2.0	0.89786	0.12174	++++
0.6	0.8	0.77297	0.26295	++++
	1.0	0.81403	0.22223	++++
	1.5	0.87745	0.15749	++++
	2.0	0.93690	0.08186	+++++
1.0	0.8	0.68023	0.57671	+++
	1.0	0.68962	0.60918	+++
	1.5	0.72545	0.61775	+++
	2.0	0.79552	0.46410	+++
1.5	0.8	0.59578	1.07305	+/−
	1.0	0.57586	1.29039	- -
	1.5	0.60673	1.37529	- -

[a] CI < 0.1: very strong synergism (+++++); CI 0.1–0.3: strong synergism (++++); CI 0.3–0.7: synergism (+++); CI 0.7–0.85: moderate synergism (++); CI 0.85–0.90: slight synergism (+); CI 0.9–1.1: nearly additive (±); CI 1.1–1.2: slight antagonism (−); CI 1.20–1.45: moderate antagonism (–).

while that of vorinostat was about 1.5 μM in 5637 (Fig. 1B). Different from 5637 cells, the cytotoxicity of vorinostat reached a plateau at 1–2.5 μM in BFTC 905 cells (Fig. 1B). For time-dependent cytotoxic analysis, it was observed that doxorubicin time- and dose-dependently reduced cell viability in 5637 and BFTC 905 cells (Fig. 1C). In the vorinostat treatment, similar levels of cytotoxicity were observed at 0.9 μM after 48 and 72 h treatment in 5637 cells. In BFTC 905 cells, cytotoxicity reached a plateau at approximately 2.5 μM after 24, 48, and 72 h treatment (Fig. 1D). According to the results of the single drug analysis, either doxorubicin or vorinostat exhibited significant cytotoxicity in 5637 and BFTC 905 cells. Therefore, the single dose of doxorubicin or vorinostat that resulted in more than 50 % cell viability after 24 h treatment was selected for drug combination analysis.

Previous studies have shown that doxorubicin and vorinostat are limited by either drug toxicity or drug resistance. Therefore, lower doses and combination therapy are required to minimize the side effects and enhance the anti-cancer effect. In the results of the combined treatment in 5637 cells, most of the CI values were lower than 0.7, indicating a moderate to strong synergistic cytotoxic effect in the combination of doxorubicin and vorinostat (Table 1 and Fig. 1E). However, it showed an antagonistic effect when a higher dose of doxorubicin was used. In BFTC 905 cells, a synergistic effect was also observed when 0.95 μM doxorubicin was used (Fig. 1E). According to the results of the combination analysis, we use the combined treatment of 5637 cells with 0.7 μM doxorubicin and 0.6 μM vorinostat, and BFTC 905 cells with 0.95 μM doxorubicin and 2 μM vorinostat (Fig. 1F). Fig. 1G shows the time-dependent cytotoxicity of combined drug treatment in 5637 and BFTC 905 cells.

The cytotoxicity of doxorubicin and vorinostat was also analyzed in a normal urothelial cell line SV-HUC-1. Using the highest concentrations used in 5637 and BFTC 905, the cell viability was still more than 65 % after 24 h treatment (Fig. 1H). In the combination of 1.5 μM doxorubicin and 5 μM vorinostat, it also presented the time-dependent cytotoxicity in SV-HUC-1 cells (Fig. 1I). Compare the cytotoxicity of single drug or combined drug treatment, more toxicity presented in 5637 and BFTC 905 than in SV-HUC-1.

3.2. *The synergistic cytotoxicity of combining doxorubicin with vorinostat induces cell death via the apoptotic pathway*

Under the combined doses of 0.7 μM doxorubicin and 0.6 μM vorinostat in 5637 cells, and 0.95 μM doxorubicin and 2 μM vorinostat

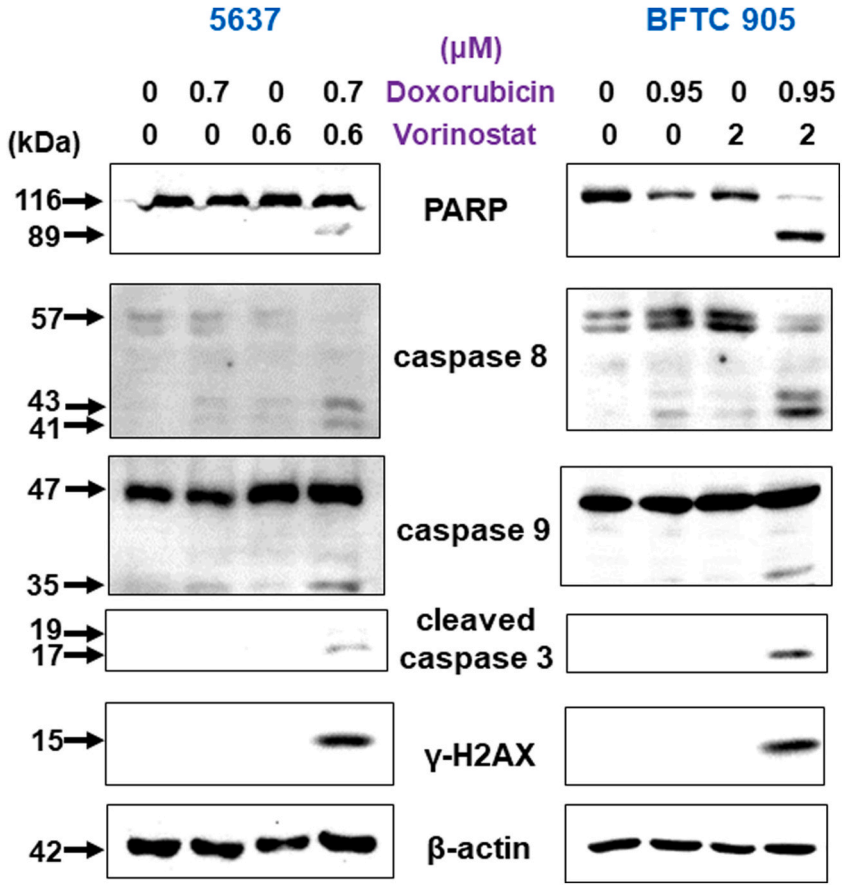

Fig. 2. The combination of doxorubicin and vorinostat induces apoptosis, and DNA strands break. 5637 and BFTC 905 cells were seeded at 3 × 10^5 cells and 4 × 10^5 cells, respectively, in a 6-cm dish and cultured for 24 h to reach 70–80 % cell confluence. Proteins were extracted after adding the doses of doxorubicin and vorinostat for another 24 h. Protein expression was analyzed by Western blot. The molecular weights of cleavage of PARP (89 kDa), caspase 8 (43 kDa and 41 kDa), caspase 9 (35 kDa), and caspase 3 (19 kDa and 17 kDa) were arrowed.

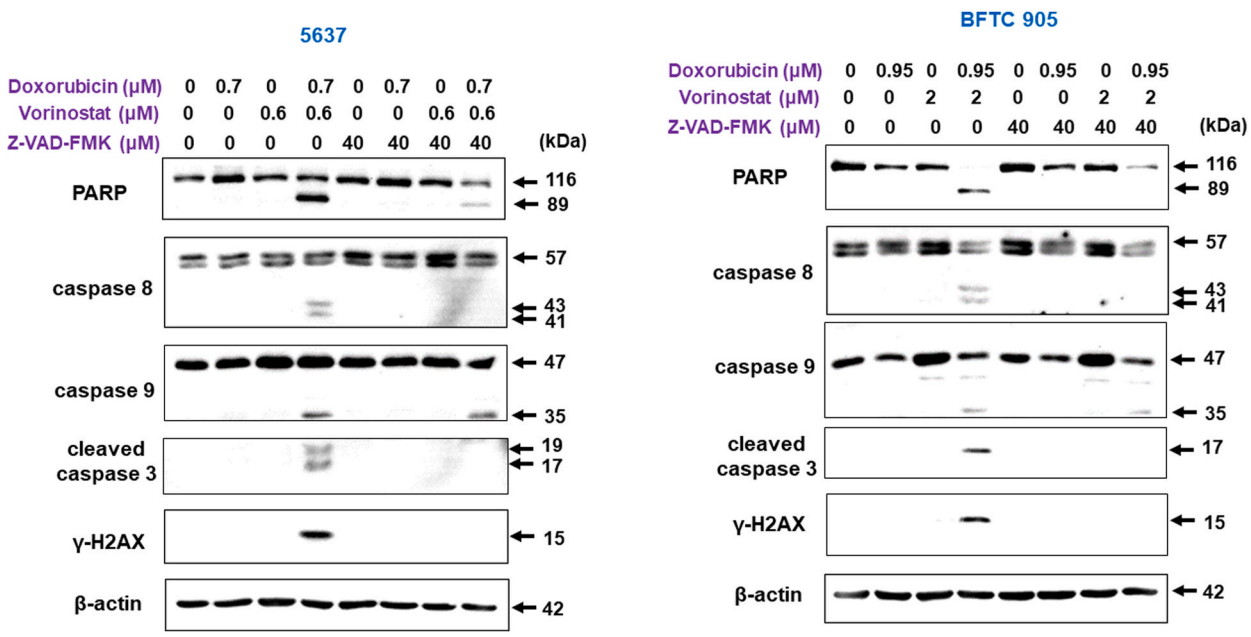

Fig. 3. Effect of Z-VAD-FMK on the combined drug-induced apoptosis-related protein expression. 5637 and BFTC 905 cells were pretreated with 40 μM Z-VAD-FMK for 1 h, then cultured with selected doses of doxorubicin and vorinostat for 24 h. Protein expression was analyzed by Western blot. The molecular weights of cleavage of PARP (89 kDa), caspase 8 (43 kDa and 41 kDa), caspase 9 (35 kDa), and caspase 3 (19 kDa and 17 kDa) were arrowed.

in BFTC 905 cells, we examined the apoptotic-related factors by Western blot. These factors included cleaved caspase-8, cleaved caspase-9, cleaved caspase-3, poly(ADP-ribose) polymerase (PARP) and a marker for DNA strand break, γ-H2AX. It shows that only the combined treatment induced significant cleavage of PARP (89 kDa), caspase 8 (43 kDa and 41 kDa), caspase 9 (35 kDa), and caspase 3 (19 kDa and 17 kDa) (Fig. 2). The combined treatment also induced γ-H2AX (15 kDa) expression, indicating that DNA strands were broken (Fig. 2). In order to confirm that the cell death was induced by apoptosis, we pretreated the cells with the pan-caspase inhibitor Z-VAD-FMK for 1 h, and then treated them with the respective doses of doxorubicin and vorinostat for 24 h. In Western blot analysis, Z-VAD-FMK inhibited the cleavage of caspase 3, caspase 8, and PARP (Fig. 3). At the same time, the protein expression of γ-H2AX was also completely inhibited. The results indicated that the protein PARP cleavage and H2AX phosphorylation were downstream of the caspase pathway. The combination of doxorubicin and vorinostat clearly induces apoptosis, suppressing the repair capability of PARP and causing DNA strand breaks by activating caspase 3. In the cell viability assay, Z-VAD-FMK restored 5637 cell viability from 46 % to 68 % in the combination drug treatment, with a recovery rate of approximately 41 % (Fig. 4A). The viability of BFTC 905 cells was restored from 30 % to 60 %, with a recovery rate of approximately 42 % (Fig. 4B). These results suggest that the caspase apoptotic pathway is involved in cell death induced by the combination of doxorubicin and vorinostat. The partial reversal of cell viability by Z-VAD-FMK also indicates that the drug combination may potentially induce other cell death mechanisms except apoptosis.

3.3. The combined treatment of doxorubicin with vorinostat induces cell death by activating the extrinsic apoptotic protein caspase 8

Caspase 8 and caspase 9 are the upstream regulators of caspase 3, primarily involved in the extrinsic death receptor and intrinsic mitochondrial pathways, respectively. Our results have shown that both cell lines activate caspase 8 and caspase 9 through combined drug treatment (Fig. 2). In Fig. 3, Z-VAD-FMK also inhibited the cleavage of caspase 8 in both cell lines but only slightly inhibited caspase 9 cleavage. In order to find out the role of caspase 8 and caspase 9 in the drug-induced cell death mechanisms, we pretreated cells with the specific caspase 8 inhibitor Z-IETD-FMK and specific caspase 9 inhibitor Ac-LEHD-CMK for 1 h, and then treated the cells with the corresponding doses of doxorubicin and vorinostat for 24 h. The results from 5637 and BFTC 905 cells showed that after pretreatment with Z-IETD-FMK, the cell viability in the combined drug treatment group showed a slight recovery of 25 % (5637) and 19 % (BFTC 905) (Fig. 5A). At the same time, cleavage of caspase 8 protein was effectively inhibited by the specific caspase 8 inhibitor in both cell lines. The 89 kDa cleavage of PARP was partially decreased, and the γ-H2AX protein was completely inhibited (Fig. 5B). In combination drug treatment, Z-IETD-FMK inhibited the cleavage 17 kDa of caspase 3 protein in 5637 and BFTC 905 cells, but the 19 kDa cleavage was not inhibited in BFTC 905 cells. On another inhibitor result, the cell viability was not restored by Ac-LEHD-CMK in both cell lines (Fig. 6A). Pretreatment with Ac-LEHD-CMK slightly reversed the cleavage of caspase 9 but didn't reverse the cleavage of caspase 3 and PARP proteins and didn't affect the phosphorylation of H2AX in both cell lines (Fig. 6B). Summarizing the results of cell viability and protein expression, it is evident that the combination of doxorubicin and vorinostat can activate caspase 3 via caspase 8 in a major and caspase 9 in a minor. Other unknown pathways are also involved in the death mechanism. Additionally, it primarily

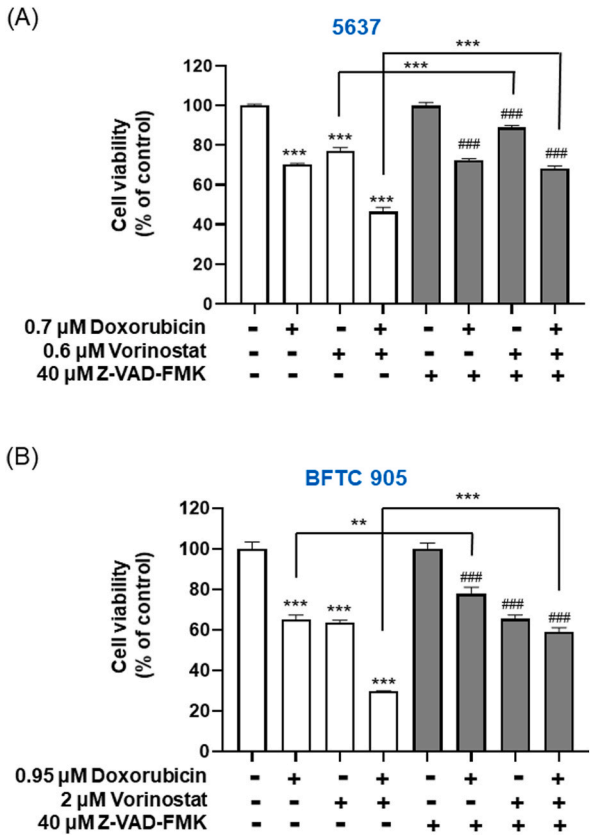

Fig. 4. Cell viability was partially restored by Z-VAD-FMK in combined drug treatment in 5637 and BFTC 905 cells. Cells were seeded on a 24-well plate and cultured for 24 h. Cells were pretreated with 40 μM Z-VAD-FMK for 1 h, then cultured with 0.7 μM doxorubicin and/or 0.6 μM vorinostat in 5637 cells (A), and 0.95 μM doxorubicin and/or 2 μM vorinostat in BFTC 905 cells (B). After 24 h treatment, cells were applied MTT assay for cell viability analysis. *** and ###$p < 0.001$, **$p < 0.01$. Symbols * and # were compared with control and Z-VAD-FMK only, respectively.

induces DNA strand breaks through caspase 8 activation in both cell lines. However, the activation of caspase 9 was not the major upstream of caspase 3, as the caspase 9 specific inhibitor could not affect the combined drugs-induced caspase 3 activation and PARP cleavage.

3.4. The combination of doxorubicin and vorinostat effectively inhibits BFTC 905 tumorspheres

BFTC 905 cell tumorsphere formation assay was simulated to mimic an in vitro tissue treatment experiment. The tumorspheres formed were treated with 0.95 μM doxorubicin, 2 μM vorinostat alone, and the combination of doxorubicin and vorinostat. This analysis was performed by counting the number of tumorspheres formed and measuring their diameter. The results differ from those of the attached cell viability assay. Only vorinostat and the combination of doxorubicin and vorinostat significantly suppressed the sphere diameter, and the combined treatment also exhibited greater toxicity than the single drug (Fig. 7).

3.5. The combination of doxorubicin and vorinostat inhibits BFTC 905 tumor growth in vivo

We further tested whether the co-treatment of doxorubicin and vorinostat has a synergistic effect in BFTC 905-inoculated xenograft mice model. The results of subcutaneous tumor growth in mice show that the combined drug treatment significantly inhibited tumor growth (Fig. 8A–C). However, weight loss was observed in the treatment groups with doxorubicin (Fig. 8D), which indicates the toxicity of doxorubicin. Among them, two mice in the doxorubicin single treatment (day 23 and day 26) and one mouse in the combined treatment group (day 24) died before reaching the endpoint (day 27). The survival rate of the 4 groups is presented in Fig. 8E. From the results, we observed a minor tumor inhibitory effect in the 1.8 mg/kg doxorubicin group without statistic significance and a significant inhibitory effect in the treatment of 1.8 mg/kg doxorubicin combined with 25 mg/kg vorinostat.

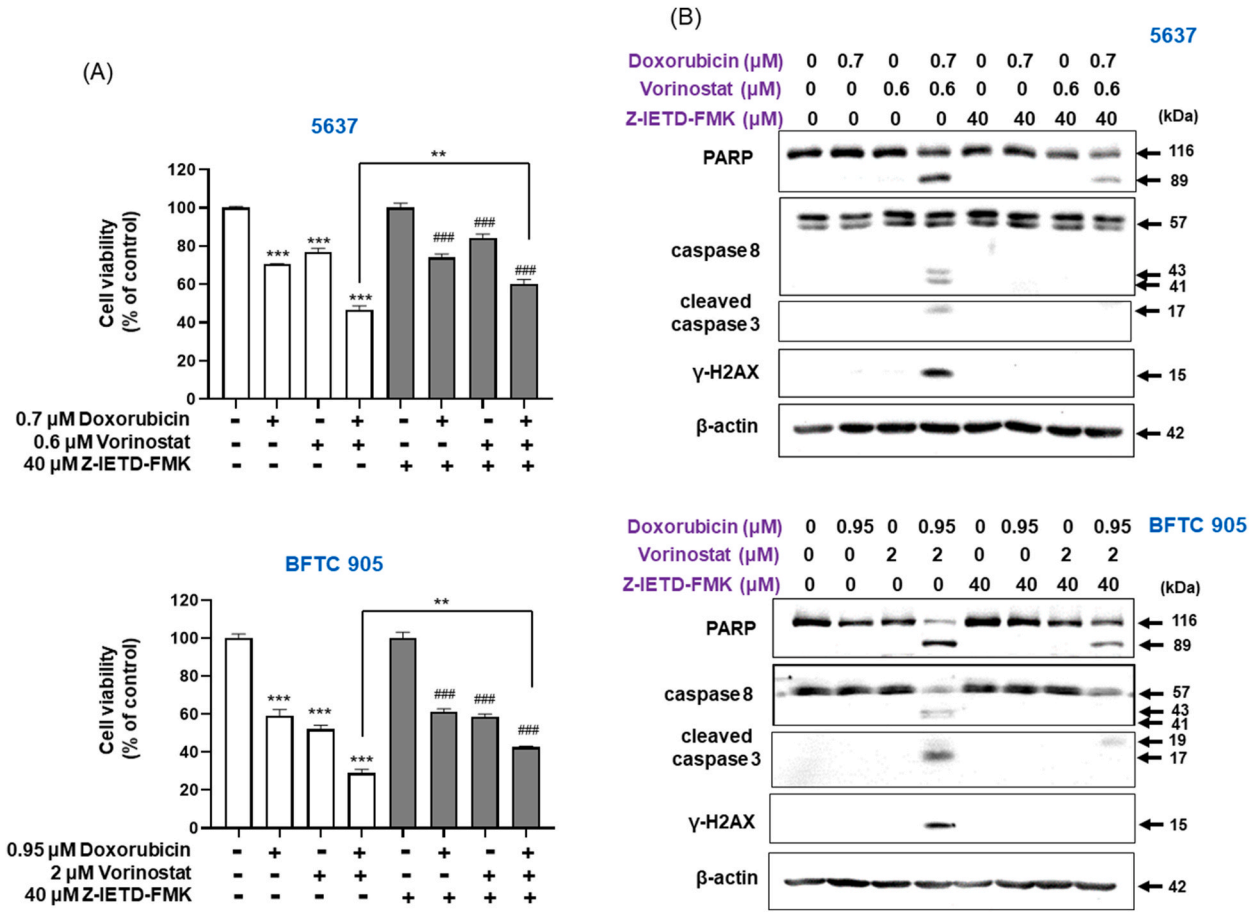

Fig. 5. Z-IETD-FMK partially restored cell viability in combined drug treatment in 5637 and BFTC 905 cells. (A) Cells were seeded on a 24-well plate and cultured for 24 h. Cells were pretreated with 40 μM Z-IETD-FMK for 1 h, then cultured with 0.7 μM doxorubicin and/or 0.6 μM vorinostat in 5637 cells and 0.95 μM doxorubicin and/or 2 μM vorinostat in BFTC 905 cells. After 24 h treatment, cells were applied MTT assay for cell viability analysis. *** and ###$p < 0.001$, **$p < 0.01$. Symbols * and # were compared with control and Z-IETD-FMK only, respectively. (B) 5637 and BFTC 905 cells were pretreated with 40 μM Z-IETD-FMK for 1 h, then cultured with selected doses of doxorubicin and vorinostat for 24 h. Protein expression was analyzed by Western blot.

4. Discussion

In summary, the most important information here is the in vivo synergistic anti-tumor effect of the combined doxorubicin and vorinostat treatment (Fig. 8). It suggests that in the future, we could consider combining doxorubicin and vorinostat for bladder cancer therapy because it might reduce the dosage and toxicity of doxorubicin. The cardiotoxicity is the most frequent side effect of doxorubicin treatment [18]. In Fig. 8, a dosage of 1.8 mg/kg of doxorubicin was administered only three times during the 10-day therapy period, yet it still resulted in the death of two mice. In the same period, a dosage of 25 mg/kg of vorinostat was injected daily for 10 days. In control and vorinostat-only groups, the mice's body weight did not decrease, and the tumor did not reduce either. No mice died in the vorinostat treatment group, but one mouse died in the combined treatment group; therefore, the drug toxicity should be attributed to doxorubicin, not vorinostat. It suggests that a combination of a reduced doxorubicin dose and a general vorinostat dose might be an effective regimen for bladder cancer therapy.

Two human bladder cell lines were used in this study. One is grade 2 urothelial carcinoma 5637, originating from a male Caucasian with primary carcinoma [19]. The other is grade 3, stage C papillary urothelial carcinoma, originating from a female of Asian descent in an area endemic to Blackfoot disease in Taiwan [20]. The morphology and growth status of the two cell lines are very different. 5637 cells are dispersed growth, while BFTC 905 cells are gathered growth in the dish. In addition, gene mutation and gene expression should differ from each other. For example, BFTC 905 exhibits wild-type p53, while the mutated p53 (R280T) is present in 5637 [20]. These variations and other unidentified distinctions may be the results of our observations in this study. In 5637 cells, vorinostat exhibits greater cytotoxicity compared to BFTC 905 cells (Fig. 1B and D). In BFTC 905 cells, the cytotoxicity of vorinostat remains at approximately 50 % after 24 h treatment, even when the concentration reaches 15 μM (Fig. 1B). Therefore, it is not appropriate to calculate CI value using Compusyn software analysis. We combined a fixed dose of vorinostat (2 μM) with three different dosages of

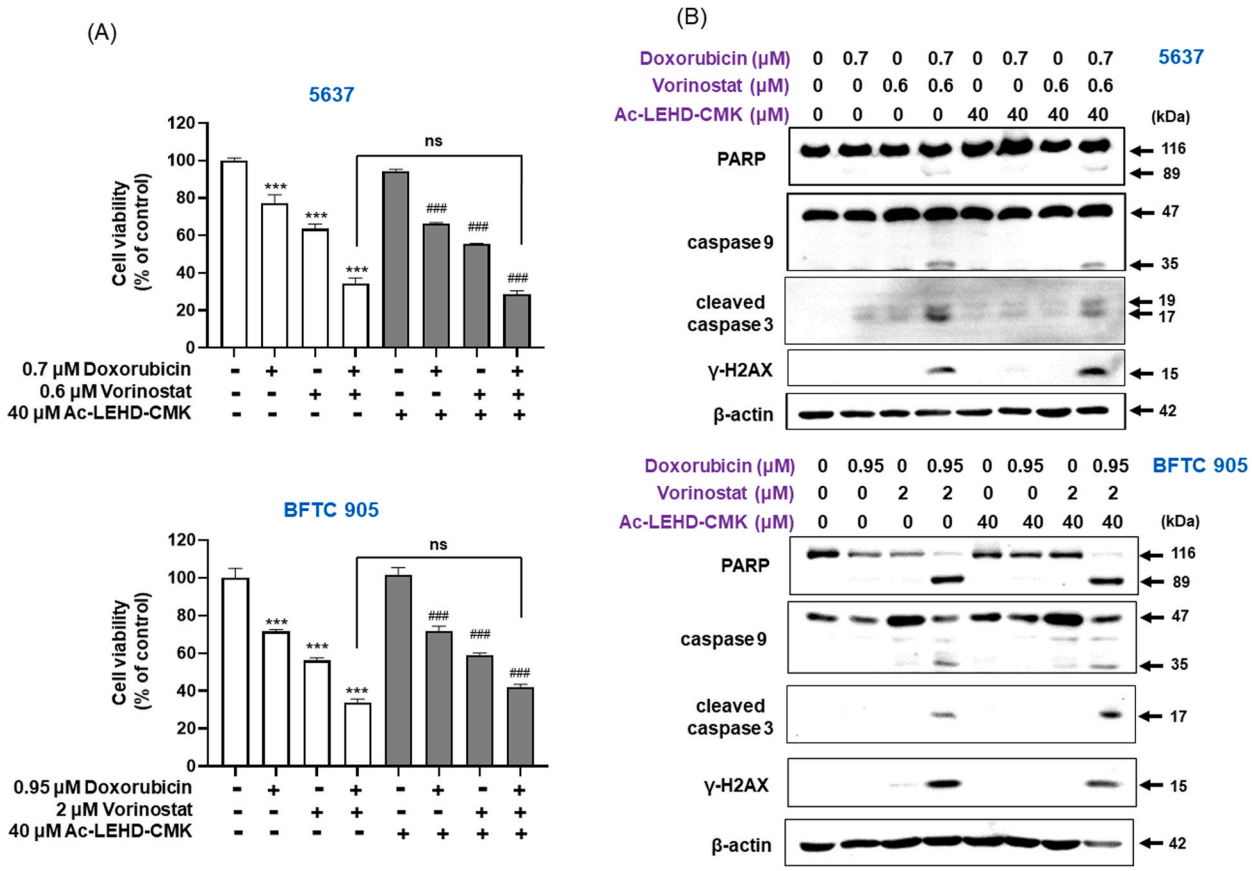

Fig. 6. Effect of Z-LEHD-FMK on the apoptotic protein expression and cell viability in combined drug treatment. (A) 5637 and BFTC 905 cells were pretreated with 40 μM Z-LEHD-FMK for 1 h, then cultured with seleted doses of doxorubicin and vorinostat for 24 h. Protein expression were analyzed by Western blot. (B) Cells were seeded on a 24-well plate and cultured for 24 h. Cells were pretreated with 40 μM Z-LEHD-FMK for 1 h, then cultured with 0.7 μM doxorubicin and/or 0.6 μM vorinostat in 5637 cells, and 0.95 μM doxorubicin and/or 2 μM vorinostat in BFTC 905 cells. After 24 h treatment, cells were applied MTT assay for cell viability analysis. *** and ###$p < 0.001$. Symbols * and # were compared with control and Z- LEHD-FMK only, respectively.

doxorubicin to determine the optimal combination dose (Fig. 1E). Although the cytotoxicity of vorinostat differs between 5637 and BFTC 905, the combined effect of doxorubicin and vorinostat is similar in both cell lines. The combination of drugs, but not a single drug, induces a significant apoptosis effect, including the cleavage of PARP, caspase 8, caspase 9, and caspase 3. It also induces a DNA double strand break signal (γHAX) (Fig. 2). The study suggests that the combination of doxorubicin and vorinostat exhibits a synergistic apoptotic effect in the two bladder cancer cell lines.

In some previous reports, it is known that vorinostat enhances doxorubicin-induced cytotoxicity in cervical cancer by upregulating Bad [21]. This combination cytotoxic effect has also been reported in rhabdoid tumor cells [22], gastric cancer [23], and some, but not all, osteosarcoma cell lines [24]. In our study, the combined cytotoxic effect is enhanced in 5637 and BFTC 905 cells through apoptosis. However, apoptosis is not the sole pathway for cell death, as evidenced by the inability of the pan-caspase inhibitor Z-VAD-FMK to reverse cell death completely (Fig. 4A). In addition, a caspase 8 specific inhibitor, Z-IETD-FMK, partially reverses PARP cleavage (Fig. 5B) and has a minor effect on reversing cell death in 5637 and BFTC 905 cells (Fig. 5A). It suggests that caspase 8 plays a partial role in the induction of apoptosis by combined drugs. However, Z-IETD-FMK, like Z-VAD-FMK, also inhibits γH2AX expression completely. This indicates that the caspase 8 pathway is responsible for the double-strand DNA breaks induced by the combined drug treatment. On the other hand, in caspase 9 specific inhibitor Ac-LEHD-CMK pretreatment, the cell viability (Fig. 6B) and γH2AX expression (Fig. 6A) of both cell lines could not be restored in combined drug treatment. It suggests that the caspase 9 pathway does not play a major role in this cell death mechanism. A study on endoplasmic reticulum (ER) stress-induced cell death found that persistent ER stress can lead to cell death through the caspase 8-apoptosis and necroptosis pathways [25]. This study reveals that caspase 8 plays a partial role in combined drug-induced apoptosis, and there are other pathways involved in the cell death mechanism. Therefore, ER stress and necroptosis may be one of the potential pathways.

In Marchion's report [15], it is suggested that vorinostat induces DNA hyperacetylation and chromatin decondensation, leading to increased DNA binding activities of topoisomerase II inhibitors, such as doxorubicin, and subsequent potentiation of DNA damage. It might be one of the synergistic mechanisms of action of the doxorubicin and vorinostat combination in this study. An earlier report

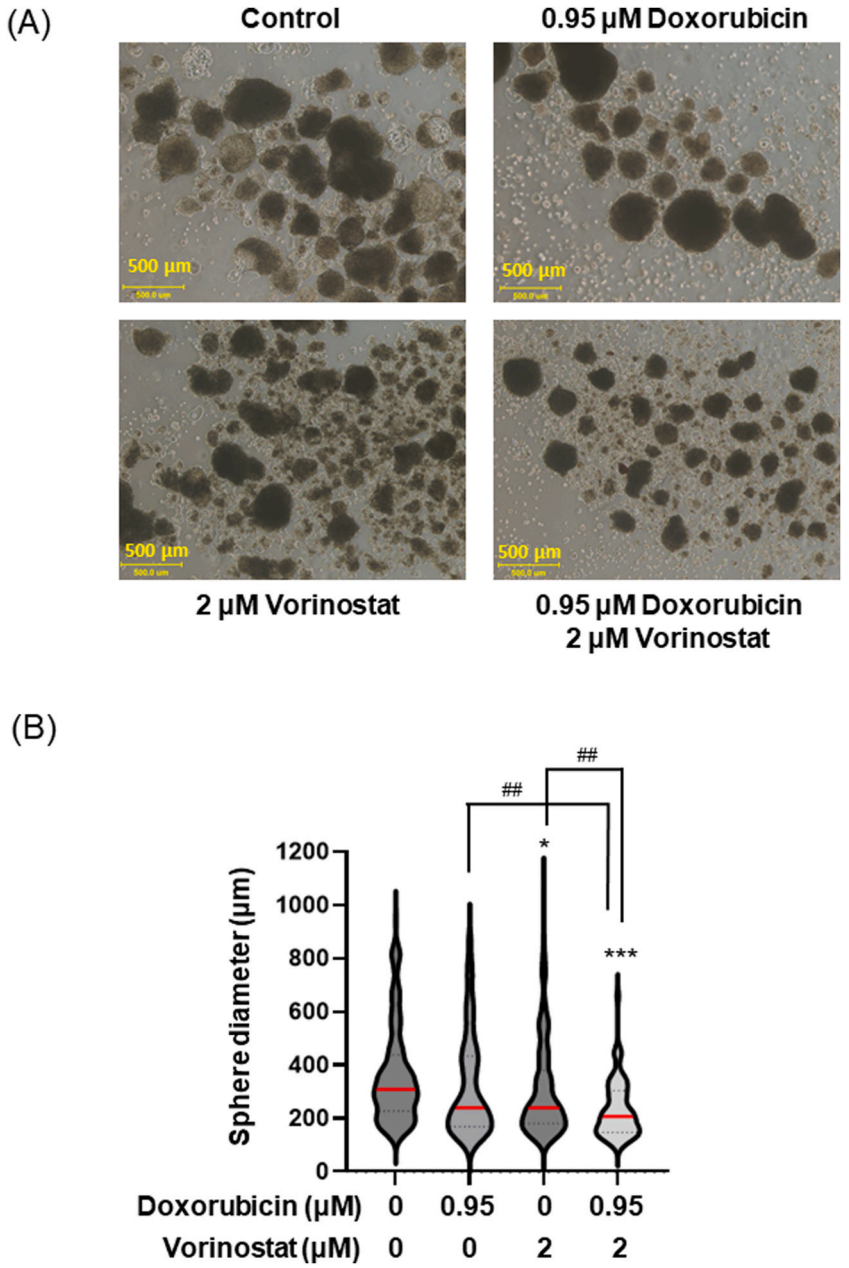

Fig. 7. Doxorubicin combined with vorinostat effectively inhibits BFTC 905 tumorspheres. BFTC 905 were cultured in 4×10^4 cells/well in 6-well plate until day 10. After tumorsphere formation, then treated with 0.95 μM doxorubicin and/or 2 μM vorinosata every 48 h for a total of 120 h. (A) Recorded by microscope after drug treatment accumulation for 120 h. The yellow scale line is 500 μm. (B) Measurement of tumorsphere diameter and statistical analysis by one-way ANOVA with Dunnett's multiple comparisons test of Prism 9. The red lines indicate median values in each group. (***$p < 0.001$ and * $p < 0.05$ compared to control, ##$p < 0.01$).

suggests that vorinostat induces cell death through transcriptional events that lead to the cleavage of Bid, disruption of the mitochondrial membrane, and generation of reactive oxygen species (ROS) [26]. In our study, we used *N*-acetylcysteine (NAC) to determine whether cell viability would be restored under single or combination treatment. The results show that NAC does not affect the cell viability of doxorubicin, vorinostat, or their combination (supplementary data). This suggests that ROS is not involved in doxorubicin-, vorinostat-, and their combination-induced cell death.

Although vorinostat exhibits cytotoxicity in cell assays (Fig. 1B), it does not have an anti-tumor effect in vivo (Fig. 8A–C). In a Phase II clinical trial, vorinostat also showed no anti-tumor effect in bladder cancer patients [12]. In a phase I trial, the combination of vorinostat and docetaxel did not demonstrate an anti-tumor effect in patients with advanced and relapsed solid malignancies [27]. In our in vivo study, the combination of vorinostat and doxorubicin demonstrates a strong anti-tumor effect in mice. Our results offer a

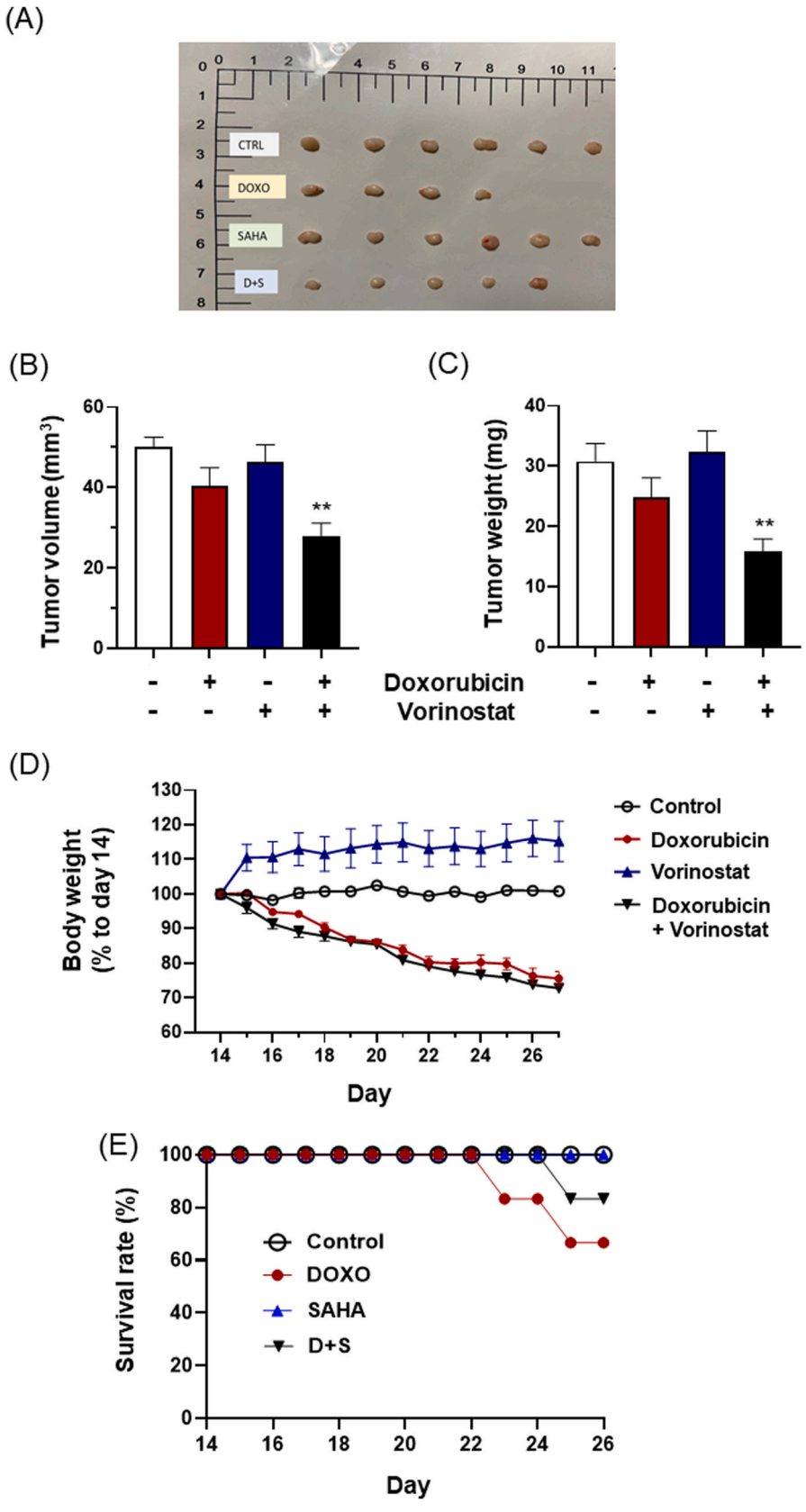

(caption on next page)

Fig. 8. Drug combination effect of doxorubicin and vorinostat in BFTC 905 xenograft mice tumor model. (A) Isolated tumor picture. CTRL: control, DOXO: doxorubicin, SAHA: vorinostat, D + S: doxorubicin and vorinostat. (B–C) Actual tumor volume (mm^3) (B) and weight (mg) (C) after removal of subcutaneous tumor after euthanized. (n = 4–6; $^{**}p < 0.01$) (D) Body weight curve of each treatment group from day 14 to day 27 using day 14 as 100 %. (E) The mouse survival rate of the four groups.

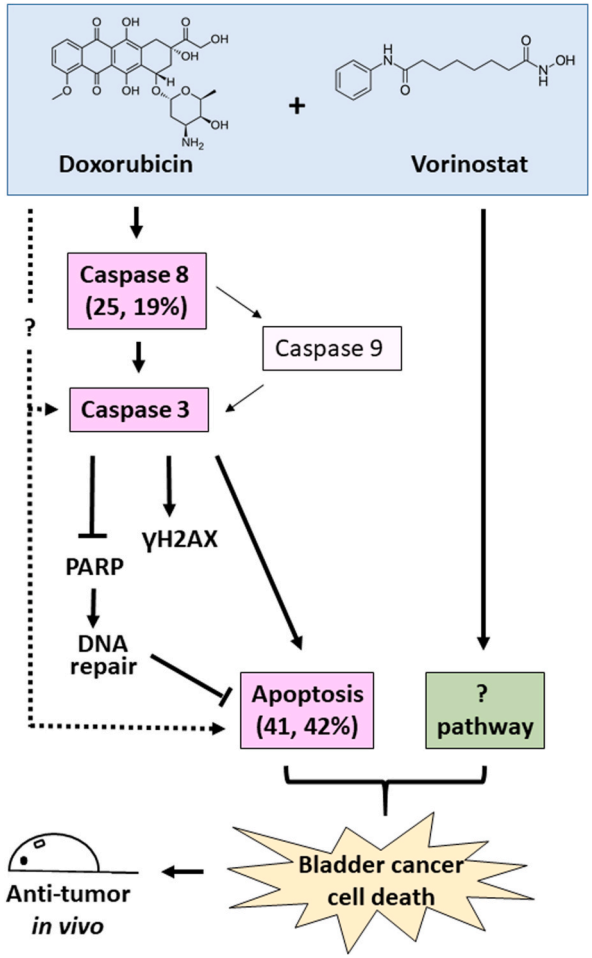

Fig. 9. Schematic mechanism illustration of doxorubicin and vorinostat combination in bladder cancers. In the combination of doxorubicin and vorinostat, it activates caspase 8-casepase3-apoptosis pathway to induce cell death. The preatment of pan-caspase inhibitors could restore a recovery rate of approximately 41 % in 5637 cells and 42 % in BFTC 905 cells. The preatment of caspase 8 specific inhibitors could restore a recovery rate of approximately 25 % in 5637 cells and 19 % in BFTC 905 cells.

practical recommendation for future urothelial carcinoma therapy, but it is still waiting to be proven in the clinic.

5. Conclusion

The combined treatment of doxorubicin and vorinostat demonstrates a synergistic anti-tumor effect on bladder cancer. The cell death mechanism of the combined doxorubicin and vorinostat is illustrated in Fig. 9. Apoptosis (pink box) and other unknown pathway (s) (green box) but not ROS are involved in the death mechanism. In the apoptosis pathway, caspase 8-caspase 3 cascade plays a significant part and might exhibit other signal(s) to the activation of caspases. In summary, the combination of doxorubicin and vorinostat could be considered for bladder cancer therapy as it may reduce the dosage and toxicity of doxorubicin.

CRediT authorship contribution statement

Cheng-Huang Shen: Writing – review & editing, Validation, Funding acquisition, Conceptualization. **Shou-Chieh Wang:** Writing – original draft, Validation, Funding acquisition. **Kah-Min Lee:** Methodology, Data curation. **Hsin-Ting Liu:** Methodology, Data curation. **Szu-Wei Huang:** Methodology. **Jin-Yi Wu:** Methodology. **Yi-Wen Liu:** Writing – review & editing, Writing – original draft,

Validation, Project administration, Methodology, Investigation, Funding acquisition, Formal analysis, Data curation, Conceptualization.

Funding

This research was supported in part by the National Science and Technology Council, Taiwan, R.O.C. (grant number NSTC112–2320-B-415-002) and SKBIO Technology Corp. (grant number Shen-1). The sponsor or funding organization had no role in the design or conduct of this research.

Declaration of competing interest

The authors declare that they have no known competing financial interests or personal relationships that could have appeared to influence the work reported in this paper.

Appendix A. Supplementary data

Supplementary data to this article can be found online at https://doi.org/10.1016/j.heliyon.2024.e41589.

References

[1] F. Bray, M. Laversanne, H. Sung, J. Ferlay, R.L. Siegel, I. Soerjomataram, A. Jemal, Global cancer statistics 2022: GLOBOCAN estimates of incidence and mortality worldwide for 36 cancers in 185 countries, CA Cancer J. Clin. 74 (2024) 229–263. https://www.ncbi.nlm.nih.gov/pubmed/38572751.
[2] A.T. Lenis, P.M. Lec, K. Chamie, M.D. Mshs, Bladder cancer: a review, JAMA 324 (2020) 1980–1991. https://www.ncbi.nlm.nih.gov/pubmed/33201207.
[3] I. Micallef, B. Baron, Doxorubicin: an overview of the anti-cancer and Chemoresistance mechanisms, Ann. Clin. Toxicol. 3 (2020) 1031.
[4] S. Rivankar, An overview of doxorubicin formulations in cancer therapy, J. Cancer Res. Therapeut. 10 (2014) 853–858. https://www.ncbi.nlm.nih.gov/pubmed/25579518.
[5] D.D. Von Hoff, M.W. Layard, P. Basa, H.L. Davis Jr., A.L. Von Hoff, M. Rozencweig, F.M. Muggia, Risk factors for doxorubicin-induced congestive heart failure, Ann. Intern. Med. 91 (1979) 710–717. https://www.ncbi.nlm.nih.gov/pubmed/496103.
[6] A. Suraweera, K.J. O'Byrne, D.J. Richard, Combination therapy with histone deacetylase inhibitors (HDACi) for the treatment of cancer: achieving the full therapeutic potential of HDACi, Front. Oncol. 8 (2018) 92. https://www.ncbi.nlm.nih.gov/pubmed/29651407.
[7] G. Li, R. Margueron, G. Hu, D. Stokes, Y.H. Wang, D. Reinberg, Highly compacted chromatin formed in vitro reflects the dynamics of transcription activation in vivo, Mol. Cell 38 (2010) 41–53. https://www.ncbi.nlm.nih.gov/pubmed/20385088.
[8] T. Eckschlager, J. Plch, M. Stiborova, J. Hrabeta, Histone deacetylase inhibitors as anticancer drugs, Int. J. Mol. Sci. 18 (2017). https://www.ncbi.nlm.nih.gov/pubmed/28671573.
[9] D. Siegel, M. Hussein, C. Belani, F. Robert, E. Galanis, V.M. Richon, J. Garcia-Vargas, C. Sanz-Rodriguez, S. Rizvi, Vorinostat in solid and hematologic malignancies, J. Hematol. Oncol. 2 (2009) 31. https://www.ncbi.nlm.nih.gov/pubmed/19635146.
[10] Y. Zhao, S. Lu, L. Wu, G. Chai, H. Wang, Y. Chen, J. Sun, Y. Yu, W. Zhou, Q. Zheng, M. Wu, G.A. Otterson, W.G. Zhu, Acetylation of p53 at lysine 373/382 by the histone deacetylase inhibitor depsipeptide induces expression of p21(Waf1/Cip1), Mol. Cell Biol. 26 (2006) 2782–2790. https://www.ncbi.nlm.nih.gov/pubmed/16537920.
[11] T.H. Lai, B. Ewald, A. Zecevic, C. Liu, M. Sulda, D. Papaioannou, R. Garzon, J.S. Blachly, W. Plunkett, D. Sampath, HDAC inhibition induces MicroRNA-182, which targets RAD51 and impairs HR repair to sensitize cells to Sapacitabine in acute myelogenous leukemia, Clin. Cancer Res. 22 (2016) 3537–3549. https://www.ncbi.nlm.nih.gov/pubmed/26858310.
[12] D.I. Quinn, D.D. Tsao-Wei, P. Twardowski, A.M. Aparicio, P. Frankel, G. Chatta, J.J. Wright, S.G. Groshen, S. Khoo, H.J. Lenz, P.N. Lara, D.R. Gandara, E. Newman, Phase II study of the histone deacetylase inhibitor vorinostat (Suberoylanilide Hydroxamic Acid; SAHA) in recurrent or metastatic transitional cell carcinoma of the urothelium - an NCI-CTEP sponsored: California Cancer Consortium trial, NCI 6879, Invest, N. Drugs 39 (2021) 812–820. https://www.ncbi.nlm.nih.gov/pubmed/33409898.
[13] H. Rikiishi, F. Shinohara, T. Sato, Y. Sato, M. Suzuki, S. Echigo, Chemosensitization of oral squamous cell carcinoma cells to cisplatin by histone deacetylase inhibitor, suberoylanilide hydroxamic acid, Int. J. Oncol. 30 (2007) 1181–1188. https://www.ncbi.nlm.nih.gov/pubmed/17390020.
[14] M.S. Kim, M. Blake, J.H. Baek, G. Kohlhagen, Y. Pommier, F. Carrier, Inhibition of histone deacetylase increases cytotoxicity to anticancer drugs targeting DNA, Cancer Res. 63 (2003) 7291–7300. https://www.ncbi.nlm.nih.gov/pubmed/14612526.
[15] D.C. Marchion, E. Bicaku, A.I. Daud, V. Richon, D.M. Sullivan, P.N. Munster, Sequence-specific potentiation of topoisomerase II inhibitors by the histone deacetylase inhibitor suberoylanilide hydroxamic acid, J. Cell. Biochem. 92 (2004) 223–237. https://www.ncbi.nlm.nih.gov/pubmed/15108350.
[16] S.E. Park, D.E. Kim, M.J. Kim, J.S. Lee, J.K. Rho, S.Y. Jeong, E.K. Choi, C.S. Kim, J.J. Hwang, Vorinostat enhances gefitinib-induced cell death through reactive oxygen species-dependent cleavage of HSP90 and its clients in non-small cell lung cancer with the EGFR mutation, Oncol. Rep. 41 (2019) 525–533. https://www.ncbi.nlm.nih.gov/pubmed/30365122.
[17] T.C. Chou, Theoretical basis, experimental design, and computerized simulation of synergism and antagonism in drug combination studies, Pharmacol. Rev. 58 (2006) 621–681. https://www.ncbi.nlm.nih.gov/pubmed/16968952.
[18] C. Belger, C. Abrahams, A. Imamdin, S. Lecour, Doxorubicin-induced cardiotoxicity and risk factors, Int. J. Cardiol. Heart Vasc 50 (2024) 101332. https://www.ncbi.nlm.nih.gov/pubmed/38222069.
[19] J. Fogh, Cultivation, Characterization, and Identification of Human Tumor Cells with Emphasis on Kidney, Testis, and Bladder Tumors, Natl. Cancer Inst. Monogr., 1978, pp. 5–9. https://www.ncbi.nlm.nih.gov/pubmed/571047.
[20] F.L. Chang, M.D. Lai, The relationship between p53 status and anticancer drugs-induced apoptosis in nine human bladder cancer cell lines, Anticancer Res. 20 (2000) 351–355. https://www.ncbi.nlm.nih.gov/pubmed/10769679.
[21] S.J. Lee, S.O. Hwang, E.J. Noh, D.U. Kim, M. Nam, J.H. Kim, J.H. Nam, K.L. Hoe, Transactivation of bad by vorinostat-induced acetylated p53 enhances doxorubicin-induced cytotoxicity in cervical cancer cells, Exp. Mol. Med. 46 (2014) e76. https://www.ncbi.nlm.nih.gov/pubmed/24525822.
[22] K. Kerl, D. Ries, R. Unland, C. Borchert, N. Moreno, M. Hasselblatt, H. Jurgens, M. Kool, D. Gorlich, M. Eveslage, M. Jung, M. Meisterernst, M. Fruhwald, The histone deacetylase inhibitor SAHA acts in synergism with fenretinide and doxorubicin to control growth of rhabdoid tumor cells, BMC Cancer 13 (2013) 286. https://www.ncbi.nlm.nih.gov/pubmed/23764045.

[23] K.S. Seah, J.Y. Loh, T.T.T. Nguyen, H.L. Tan, P.E. Hutchinson, K.K. Lim, B.W. Dymock, Y.C. Long, E.J.D. Lee, H.M. Shen, E.S. Chen, SAHA and cisplatin sensitize gastric cancer cells to doxorubicin by induction of DNA damage, apoptosis and perturbation of AMPK-mTOR signalling, Exp. Cell Res. 370 (2018) 283–291. https://www.ncbi.nlm.nih.gov/pubmed/29959912.

[24] A. Pettke, M. Hotfilder, D. Clemens, S. Klco-Brosius, C. Schaefer, J. Potratz, U. Dirksen, Suberanilohydroxamic acid (vorinostat) synergistically enhances the cytotoxicity of doxorubicin and cisplatin in osteosarcoma cell lines, Anti Cancer Drugs 27 (2016) 1001–1010. https://www.ncbi.nlm.nih.gov/pubmed/27487911.

[25] R. Iurlaro, C. Munoz-Pinedo, Cell death induced by endoplasmic reticulum stress, FEBS J. 283 (2016) 2640–2652. https://www.ncbi.nlm.nih.gov/pubmed/26587781.

[26] A.A. Ruefli, M.J. Ausserlechner, D. Bernhard, V.R. Sutton, K.M. Tainton, R. Kofler, M.J. Smyth, R.W. Johnstone, The histone deacetylase inhibitor and chemotherapeutic agent suberoylanilide hydroxamic acid (SAHA) induces a cell-death pathway characterized by cleavage of Bid and production of reactive oxygen species, Proc. Natl. Acad. Sci. U.S.A. 98 (2001) 10833–10838. https://www.ncbi.nlm.nih.gov/pubmed/11535817.

[27] B.J. Schneider, G.P. Kalemkerian, D. Bradley, D.C. Smith, M.J. Egorin, S. Daignault, R. Dunn, M. Hussain, Phase I study of vorinostat (suberoylanilide hydroxamic acid, NSC 701852) in combination with docetaxel in patients with advanced and relapsed solid malignancies, Invest. N. Drugs 30 (2012) 249–257. https://www.ncbi.nlm.nih.gov/pubmed/20686817.